RSC Advances

PAPER

View Article Online
View Journal | View Issue

Cite this: *RSC Adv.*, 2024, **14**, 6865

Flexible thermoelectric CMTs/KCl/gelatin composite for a wearable pressure and temperature sensor†

Hongjie Wang,[a] Jilun Guan,[a] Mei He,*[a] Yanqiu Zhu *[c] and Fangchao Cheng *[ab]

Received 11th December 2023
Accepted 12th February 2024

DOI: 10.1039/d3ra08471j

rsc.li/rsc-advances

Flexible sensors have promising applications in the fields of health monitoring and artificial intelligence, which have attracted much attention from researchers. However, the design and manufacture of sensors with multiple sensing functions (like simultaneously having both temperature and pressure sensing capabilities) still present a significant challenge. Here, an ionic thermoelectric sensor for synchronous temperature and pressure sensing was developed on the basis of a carbon microtubes (CMTs)/potassium chloride (KCl)/gelatin composite consisting of gelatin as the polymer matrix, CMTs as the conductive material and KCl as the ion source. The designed CMTs/KCl/gelatin composite with the good ductility (830%) and flexibility can achieve a Seebeck coefficient of 4 mV K^{-1} and a dual stimulus responsiveness to pressure and temperature. In addition, not only the movement of the human body (*e.g.*, fingers, arms), but also the temperature difference between the human body and the environment, were able to be monitored by the designed CMTs/KCl/gelatin sensors. This study provides a novel strategy for the design and preparation of high-performance flexible sensors by utilizing ion-gel thermoelectric materials and promotes the research of temperature and pressure sensing technologies.

1 Introduction

In recent years, flexible sensors[1–3] have attracted great interest due to their great potential in health monitoring[4] and smart electronic devices.[5] For example, flexible electronic sensors can convert physiological activity signals into visible electrical signals through signal conduction, which has great application prospects in the fields of human clinical diagnosis, human–computer interaction,[6] artificial intelligence robotics,[7] and flexible electronic skin.[8–10] In particular, flexible sensors can be used for multifunctional sensing, such as pressure and temperature sensing,[11–15] through the thermoelectric, piezoelectric, and friction electric properties of the materials. Ionic gels with dual stimulated temperature and pressure responsive materials are expected to provide an idea for the construction of temperature and pressure sensors.

The ionic gel can be used as thermoelectric material that relies on the thermal diffusion effect of ions and the thermal current effect of ions for thermal-electric conversion.[16] Meanwhile, the ionic gel provide a new way for temperature sensing by using the thermal diffusion effect of ions to generate a potential difference. Based on the advantages of high thermoelectric properties, low preparation cost and good tensile properties, the ionic gel have a wide range of applications in energy storage and energy conversion.[17] Furthermore, the ionic thermoelectric gel material generates a corresponding potential difference due to the thermal diffusion of ions in the ionic gel that results in the accumulation of ions at the two ends of the sample to produce an ionic concentration gradient. Furthermore, due to the thermal diffusion of ions in the ionic gel, the ionic gel generates a corresponding potential difference, leading to the aggregation of ions at the two ends of the sample to produce an ionic concentration gradient. Therefore, ions (*e.g.*, KCl, NaCl)[18] were introduced into the ionic gel to improve the thermoelectric and electrical conductivity of ionic gels, such as low-cost, environmentally friendly salt solutions. However, the present ionic gel has many disadvantages, such as easy volatility, leakage, poor mechanical properties and low thermoelectric properties, limiting their application in flexible sensor devices.

In order to obtain high-performance ionic thermoelectric gel materials, conductive materials and fillers (*e.g.*, PSSH, PEDOT:PSS, and PSSA)[19–21] are invariably introduced to improve the mechanical strength, thermoelectric properties, and

[a]*State Key Laboratory of Featured Metal Materials and Life-cycle Safety for Composite Structures, School of Resources, Environment and Materials, Guangxi University, Nanning 530004, China. E-mail: meihe@gxu.edu.com; fangchaocheng@gxu.edu.cn*

[b]*College of Material Science and Engineering, Central South University of Forestry and Technology, Changsha 410004, China*

[c]*College of Engineering, Mathematics and Physical Sciences, University of Exeter, Exeter EX4 4QF, UK. E-mail: Y.Zhu@exeter.ac.uk*

† Electronic supplementary information (ESI) available: Figures of the structural characterization of CMTs and KCl/gelatin. In addition, the comparison of the CMTs/KCl/gelatin sensor with other materials and Seebeck coefficient and conductivity of gels with different components are also included in the ESI. See DOI: https://doi.org/10.1039/d3ra08471j

structural stability of ionic thermoelectric gel materials. Carbon nanomaterials possess high electrical conductivity, large specific surface area, and tunable chemical composition and structure, which make them stand out among many other conductive materials. As a carbon nanomaterial, carbon nanotubes (CNTs), have high strength,[22,23] high electrical conductivity,[24,25] high thermal conductivity,[26,27] and excellent chemical stability properties.[28,29] Carbon microtubes (CMTs) have a larger tubular structure in addition to the similar properties of carbon nanotubes. Moreover, CMTs possesses relatively stable chemical properties and high specific surface area,[30] which can serve as a stable ionic carrier and channel in ionic gel material. Hence, CMTs are the potential conductive material to prepare ionic thermoelectric gel materials with good thermoelectric properties, non-toxicity, flexible stretchability, temperature sensitivity and pressure sensitivity.

In this work, we reported a dual-mode flexible sensor for temperature and pressure based on ionic thermoelectric gel material. CMTs/KCl/gelatin composite was prepared by a facile dissolution process using gelatin, CMTs and KCl. The Seebeck coefficient of the prepared ionic gel was 4 mV K^{-1} at KCl concentration of 0.8 M, the gelatin fraction of 30 wt% and the CMTs addition of 30 mg. Then, CMTs/KCl/gelatin composite with thermoelectric effect was utilized to develop flexible thermal sensors capable of simultaneous monitoring of temperature and pressure. Accordingly, the obtained CMTs/KCl/gelatin flexible sensor with the multifunctional sensing properties have great potentials in the field of human–computer interaction, wearable electronic devices and electronic skin.

2 Experimental

2.1 Materials

Gelatin, chitosan, sodium dodecylbenzene sulphonate (SDBS) and choline chloride were purchased from Shanghai Aladdin Biochemical Science and Technology Co., Ltd. Potassium chloride, sodium chloride, ferric nitrate and oxalic acid were obtained from Tianjin Damao Chemical Reagent Factory.

2.2 Preparation of CMTs solution

0.1 g CMTs were dispersed in 20 mL of deionized water, and then 0.1 g of sodium dodecylbenzene sulphonate (SDBS) was added as surfactant to obtain the CMTs mixture. Next, 5 mL of HCl was added to the CMTs mixture to functionalize CMTs. Subsequently, the prepared CMTs mixture was subjected to ultrasonic treatment for 2 h in an ultrasonic cleaner.

2.3 Preparation of CMTs/KCl/gelatin composite

Ionic gels were prepared by mixing gelatin, CMTs and KCl. Firstly, gelatin, CMTs and KCl were added in deionized (DI) water of 10 mL. The detailed compositions of various ionic gels and the effects of compositions on the thermoelectric properties are shown in Fig. S1.† The solution was stirred at 60 °C for at least 4 h until a homogenous solution was formed. Subsequently, the ionic gel was poured into a mold for cooling and forming, and the cured gel was taken out and dried in air at room temperature for 4 h to achieve the suitable moisture content. The prepared ionic gel was named as CMTs/KCl/gelatin composites. In addition, the gelatin and KCl/gelatin composite were prepared in the same way for subsequent comparative analysis.

2.4 Characterization

The CMTs/KCl/gelatin composite was first frozen in a cold trap at −55 °C, and then freeze-dried under vacuum at −64 °C for 24 h. The morphology of the freeze-dried hydrogel sample was observed by scanning electron microscopy (SEM; Sigma300, Zeiss, German) at 5 kV for secondary electron imaging after being coated with gold. FTIR spectra of the CMTs/KCl/gelatin composite was acquired using a Nicolet 6700 infrared spectrometer (Thermo Fisher Scientific Corp, USA) in the 1000–4000 cm^{-1} wavenumber range.

Tensile tests were carried out at room temperature using a universal testing machine (Instron 5967). The dimensions of the tensile specimens were 40 mm × 10 mm × 1 mm. Five specimens were performed on each sample and the results were averaged.

The Seebeck coefficient of the ionic thermoelectric gel electrolyte was specifically tested by using Peltier elements to control the temperature of the cooler and heater. Then the electrochemical workstation was used to measure the open circuit voltage on both sides of the CMTs/KCl/gelatin composite electrolyte, and the thermocouple K-type thermocouple thermometer was used to measure the real-time temperature at both ends of the electrolyte. The formula for the calculation of Seebeck coefficient is given below:

$$S = \frac{V_h - V_c}{T_h - T_c} \quad (1)$$

where S is the Seebeck coefficient, V_h and V_c are the voltage are the temperatures at the hot electrode and the cold electrode, T_h and T_c are the temperatures at the hot electrode and the cold electrode, respectively.

3 Results and discussion

3.1 Preparation mechanism of the CMTs/KCl/gelatin composite

A schematic diagram of the preparation process of the CMTs/KCl/gelatin composite by a mixed dissolution method is shown in Fig. 1. First, CMTs were formed by high-temperature carbonization using a mixed system of biomass, ionic liquids and low-eutectic solvents as a carbon source in the presence of Fe^{3+} as a catalyst. In Fig. S2,† it is shown that the CMTs has a graphitic structure from the XRD spectra and Raman spectra. From the figure, it can be seen that the CMTs have a strong G peak, a relatively weak D peak and a large ratio of I_D/I_G, which indicates that the CMTs are highly graphitized. In addition, the CMTs have a high electrical conductivity, indicating superior electrical conductivity. Due to the presence of nitrogen in the hybrid system, nitrogen element was also present in the structure of the synthesized CMTs in Fig. S2.† The presence of

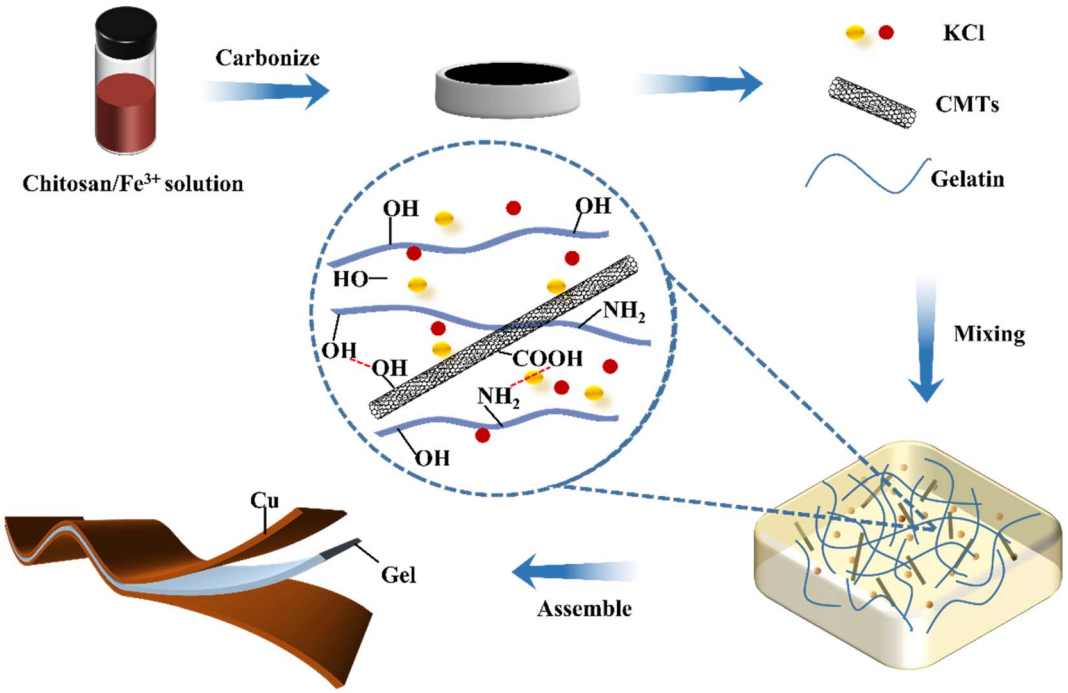

Fig. 1 Schematic diagram for the CMTs/KCl/gelatin composite preparation.

nitrogen element was beneficial to improve the electrical conductivity of CMTs and enhance their structural stability and mechanical strength. Then, the CMTs/KCl/gelatin composite was obtained by mixing gelatin and KCl thoroughly at 60 °C and further cooling the co-mixed system to room temperature. Finally, CMTs/KCl/gelatin composite were assembled as a flexible sensor by adhering copper sheets on both sides of the gels and copper sheets were used as electrodes. Moreover, the incorporation of CMTs in the gelatin network could facilitate the improvement of the thermoelectric properties of the gels. The interface interaction between CMTs and gelatin network could enhance the internal structure of the CMTs/KCl/gelatin composite, further improving the flexibility of the CMTs/KCl/gelatin composite.

3.2 Structural analysis of the CMTs/KCl/gelatin composite

Fig. 2(a) shows the macroscopic morphology of the synthesized CMTs. It can be seen that the synthesized CMTs presents an aerogel-like structure and the individual CMTs possess a long aspect ratio, which could be beneficially incorporated into the CMTs/KCl/gelatin composite to obtain a lightweight, low-density and soft conductive networks. As shown in Fig. 2(b), the synthesized CMTs microtubes had a maximum length of 10 μm with a tube diameter of 500 nm. Also, the obtained CMTs showed a morphology of bamboo-joints, and the raised portion could greatly increase the surface roughness and specific surface area of the CMTs. This bamboo-joints structure could enhance the contact interface between CMTs and gel matrix as well as the adsorption of ions by the CMTs in Fig. 2(c), resulting in obtaining high-performance the CMTs/KCl/gelatin composite. As shown in Fig. S3,† the microstructure of the KCl/gelatin composite has a rough surface and the precipitated KCl is uniformly distributed on the surface of the composite. Fig. 2(d) show the microscopic morphology that CMT was successfully doped in the CMTs/KCl/gelatin composite structure and the CMTs/KCl/gelatin composite possesses abundant pore structures. Additionally, CMTs were wrapped with gelatin and shuttled into the gaps of the gel matrix, which was beneficial to improve the mechanical and electrical conductivity of the CMTs/KCl/gelatin composite. Moreover, the incorporated N and Fe elements were uniformly distributed in the CMTs in Fig. 2(e)–(h), which was helpful to promote the ionic mobility and electrical conductivity inside the CMTs/KCl/gelatin composite.[31]

The FTIR spectrum of the CMTs/KCl/gelatin composite and KCl/gelatin composite is presented in Fig. 2(i). In the FTIR spectrum of the CMTs/KCl/gelatin composite, the peak at 1633 cm^{-1} was attributed to the amide I band (C=O) stretching vibration of the gelatin molecule, the peak at 1536 cm^{-1} was attributed to the bending vibration of its amide II band (N–H) and the peak at 1242 cm^{-1} was attributed to the amide III band (C–H) stretching vibration.[32,33] The CMTs/KCl/gelatin composite had a broad absorption peak at 3305 cm^{-1}, which was the –OH stretching vibration of the CMTs/KCl/gelatin composite.[34] Moreover, the CMTs/KCl/gelatin composite incorporated showed two peaks about 2926 cm^{-1} and 2854 cm^{-1}, associating with the stretching vibration of CMTs $-CH_2$ group.[35]

3.3 Mechanical properties of the CMTs/KCl/gelatin composite

Flexibility properties was one of the most important performances of flexible sensors, directly affecting the wearability,

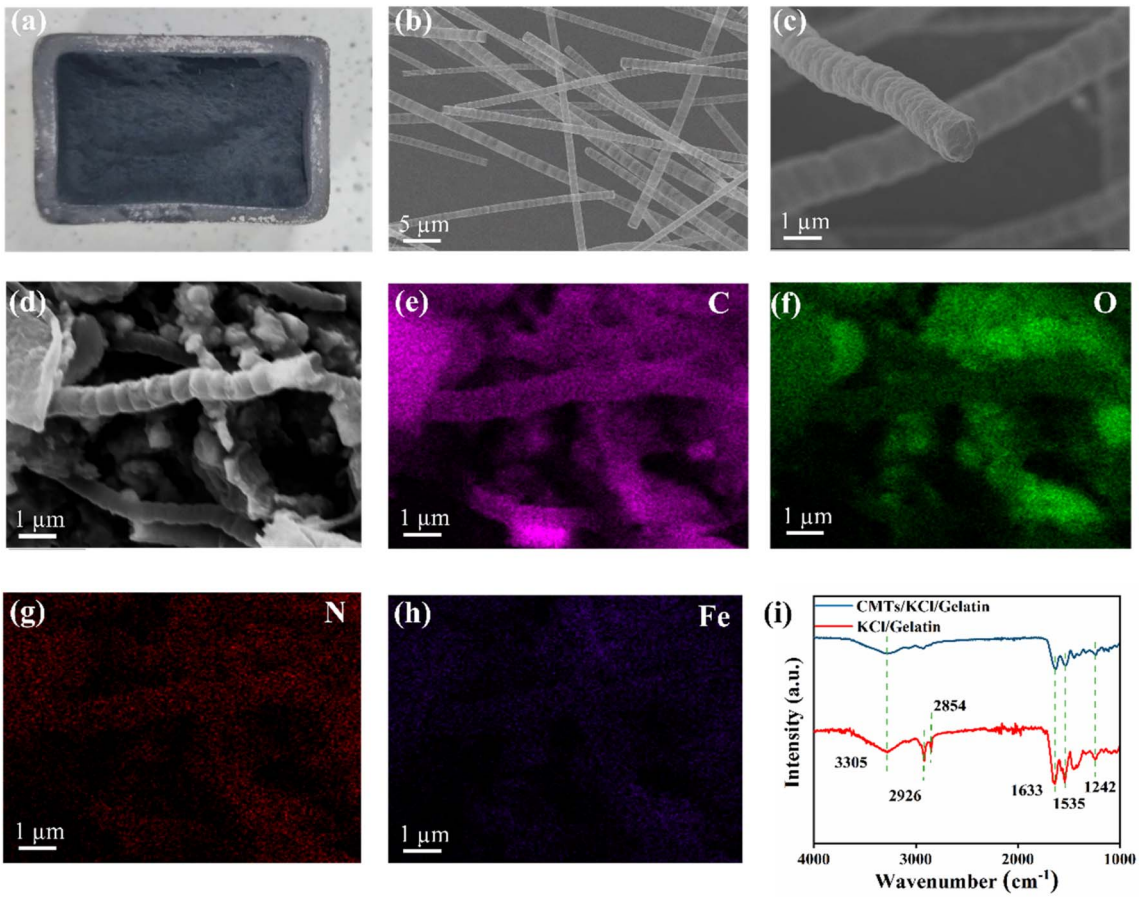

Fig. 2 Structural characteristics of the CMTs/KCl/gelatin composite. (a) Macroscopic morphology of CMTs, (b and c) SEM images of CMTs, (d) SEM images of the CMTs/KCl/gelatin composite. (e–h) EDS energy spectra of the CMTs/KCl/gelatin composite. (i) FTIR spectra of KCl/gelatin and CMTs/KCl/gelatin composite.

reliability and durability of the sensor's sensing performance. In order to evaluate the flexibility of the CMTs/KCl/gelatin composite, the stretching, twisting and bending tests of the CMTs/KCl/gelatin composite were conducted. As been shown in Fig. 3(a), the CMTs/KCl/gelatin composite could be stretched from 4 cm to 8 cm without breaking and could be easily folded and bent without cracking, displaying excellent toughness and flexibility properties. In addition, the mechanical properties of the CMTs/KCl/gelatin composite with different KCl concentrations, mass fraction of gelatins and additions of CMTs were further quantified with tensile testing in Fig. S4.† With the increase of the of KCl concentrations, the mechanical properties of the CMTs/KCl/gelatin composite appeared the decreasing trend in Fig. 3(b). Owing to the fact that the addition of KCl could improve the thermoelectric properties of the CMTs/KCl/gelatin composite,[36] KCl concentration of 0.8 M was the better choice after considering the mechanical and thermoelectric properties of the CMTs/KCl/gelatin composite. As shown in Fig. 3(c), the tensile strength and elongation at break of the CMTs/KCl/gelatin composite were increased significantly with the increase of mass fraction of gelatins. This phenomenon was due to the abundance reactive groups in gelatin, which could combine with the groups on the surface of CMTs so as to improve the mechanical properties of the CMTs/KCl/gelatin composite. Meanwhile, with the additions of CMTs increased from 10 mg to 40 mg, the tensile strength of the CMTs/KCl/gelatin composite obviously increased from 0.55 MPa up to 1.7 MPa and the elongation at break monotonically increased from 460% to 1200% owing to the large aspect ratio of CMTs in Fig. 3(d).[37]

3.4 Thermoelectric properties of the CMTs/KCl/gelatin composite

The temperature sensing of the CMTs/KCl/gelatin composite was based on the thermal diffusion effect of the CMTs/KCl/gelatin composite, thus the study of the thermoelectric properties of the CMTs/KCl/gelatin composite could contribute to optimize their temperature sensing performance and improve the sensing accuracy. The Seebeck coefficient of the CMTs/KCl/gelatin composite prepared from pure gelatin was 0.56 mV K^{-1} in Fig. S1.† After the addition of KCl and CMTs to gelatin, the Seebeck coefficient and conductivity of CMTs/KCl/gelatin composites were significantly increased as shown in Fig. S1.† The cation thermal mobility was greater than the anion thermal mobility in the CMTs/KCl/gelatin composite.[38] Therefore, the cold side of the CMTs/KCl/gelatin composite could assemble

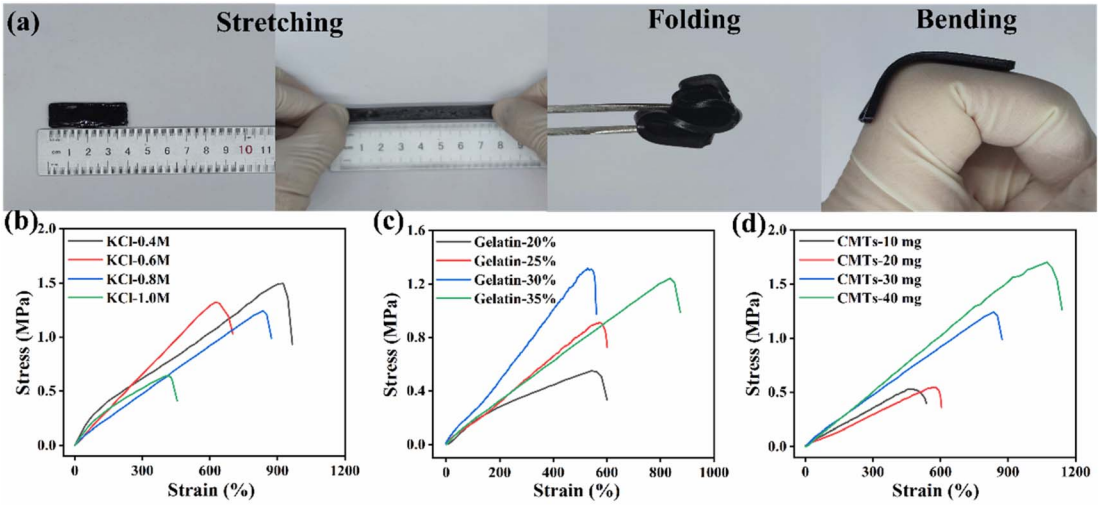

Fig. 3 Mechanical properties of the CMTs/KCl/gelatin composite. (a) Stretching and twisting of the CMTs/KCl/gelatin composite. Stress–strain curves of the CMTs/KCl/gelatin composite with (b) different KCl concentrations, (c) different mass fraction of gelatin and (d) different additions of CMTs.

more K^+ compared to Cl^-, resulting in net positive and negative charge densities near the cold and hot electrodes,[39] respectively. The distribution of these net charge densities could induce a built-in electric field pointing from the cold side to the hot side, resulting in a voltage. Thus, the Seebeck coefficients of the CMTs/KCl/gelatin composite were evaluated with different KCl concentrations. As the increase of KCl concentration, the contents of movable cations in the CMTs/KCl/gelatin composite were increased subsequently, resulting in the increase in the Seebeck coefficient of the CMTs/KCl/gelatin composite in Fig. 4(a) and (b). However, the Seebeck coefficient showed a decrease as the KCl concentration increased from 0.8 M to 1 M. This was caused by the fact that KCl could weaken the Debye length of the polymer surface charge when the concentration of KCl was too large, and the result tends to the value of the Seebeck coefficient of the pure KCl solution.[40] In addition,

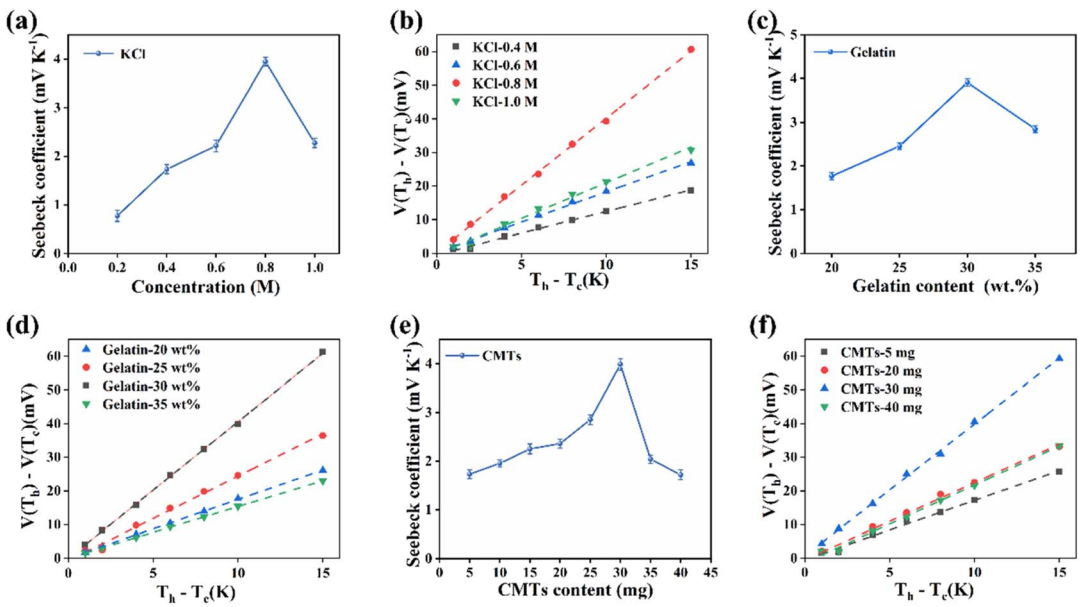

Fig. 4 Thermoelectric properties of the CMTs/KCl/gelatin composite. (a) Seebeck coefficients of the CMTs/KCl/gelatin composite with different KCl concentrations. (b) Thermal voltages of the CMTs/KCl/gelatin composite with different KCl concentrations for each temperature gradient. (c) Seebeck coefficients of the CMTs/KCl/gelatin composite with different mass fraction of gelatins. (d) Thermal voltages of the CMTs/KCl/gelatin composite with different mass fraction of gelatins for each temperature gradient. (e) Seebeck coefficients of the CMTs/KCl/gelatin composite with different CMTs additions. (f) Thermal voltages of the CMTs/KCl/gelatin composite with different CMTs additions for each temperature gradient temperature gradient.

the Seebeck coefficients of the CMTs/KCl/gelatin composite could increase from 1.75 mV K^{-1} to 4 mV K^{-1} by varying the mass fraction of gelatins in the CMTs/KCl/gelatin composite in Fig. 4(c) and (d). The Seebeck coefficients of CMTs/KCl/gelatin composites are higher than those of many reported materials according to Table S1.† However, excess gelatin could lead to a reduction of water in the CMTs/KCl/gelatin composite, inhibiting the mobility of ions and the thermo-electric properties of the CMTs/KCl/gelatin composite.

Furthermore, the Seebeck coefficients of gels with different CMTs additions were measured to assess the effect of CMTs on the thermoelectric properties of the CMTs/KCl/gelatin composite. As shown in Fig. 4(e) and (f), the Seebeck coefficients of the CMTs/KCl/gelatin composite could firstly increase as the addition of CMTs increased and then showed a decreasing trend, reaching the peak after the addition of 30 mg CMTs. This was because the prepared CMTs were obtained after strong acid treatment, which could increase the activation degree of the CMTs surface groups (*e.g.*, –OH and –COOH, *etc.*). The increased activation degree could cause an increase in the concentration difference between cations and anions in the CMTs/KCl/gelatin composite,[41,42] resulting in an increase in the Seebeck coefficient. Moreover, the obtained CMTs were doped with N and Fe elements in Fig. 2(g) and (h), which could enter into the interstitial and defective sites of the CMTs. That was to say, the presence of N and Fe elements could enhance the charge transfer and storage capacity of the CMTs, thereby improving the thermoelectric properties of the CMTs/KCl/gelatin composite. However, with the addition of CMTs to a certain extent, the CMTs in the CMTs/KCl/gelatin composite appeared to aggregate. The aggregation of CMTs could affect the ions transport of the CMTs/KCl/gelatin composite, thereby affecting the thermoelectric properties of the system. Meanwhile, the aggregation of CMTs also could inhibit the formation of the CMTs/KCl/gelatin composite and decrease the stability of the composite structure.

3.5 The CMTs/KCl/gelatin sensor applications

The CMTs/KCl/gelatin composite possessed stable thermoelectric properties, making ideal materials for temperature sensors. Consequently, the CMTs/KCl/gelatin composite was assembled as a temperature sensor to explore their potential application in human body temperature detection in Fig. 5(a), and the CMTs/KCl/gelatin composite was used as electrolytes and copper foils as electrodes. The temperature sensing mechanism of the sensor is shown in Fig. 5(b). Based on the thermal diffusion effect, the anions and cations in the CMTs/KCl/gelatin composite were driven to move by the difference in temperature between the two ends. The asynchronous movement of the anions and cations resulted in a homogeneous distribution of ions in the composite, leading to the formation of a potential difference between the two ends of the sensor. Thus, the CMTs/KCl/gelatin sensor could provide an indication of the thermal condition of the sensing region. As shown in Fig. 5(d), the CMTs/KCl/gelatin sensor exhibits uniform voltage changes when different temperature differences were applied on both sides of the sensor, indicating excellent stability of the CMTs/KCl/gelatin sensor. When the temperature difference between the two sides was cancelled, the voltage on both sides of the sensor would return to the original value and the sensor showed good responsiveness to temperature changes. Moreover, the sensor voltage was positively correlated with the temperature difference between the two sides. That was to say, the greater the temperature difference, the higher the sensor voltage. In addition, the sensor also could generate a stable voltage change based on the temperature difference between the skin and the air in Fig. 5(e). According to the Seebeck coefficient of the CMTs/KCl/gelatin composite, the voltage generated by the temperature difference between the two sides of the sensor was similar to the actual voltage value measured on both sides of the sensor, indicating that the sensor could accurately detect the temperature difference between the two sides of the sensor in Fig. 5(c). Thickness of the CMTs/KCl/gelatin composite was the important factor on temperature sensing. At temperature difference of 1 K, the thicker the thickness, the greater the voltage change and the higher the sensitivity of the sensor in Fig. 5(f).

To further verify the reliability of the CMTs/KCl/gelatin composite in temperature sensing, the temperature sensing of the palm of the hand in non-contact with the sensor was measured. The palm was placed at a distance of 1 cm above the sensor, and the temperature on both sides of the sensor was monitored by thermal imaging technology in Fig. 5(g). The voltage response was successfully obtained in Fig. 5(h). The temperature difference measured by the thermal imaging technique was 0.8 K, which was essentially the same as the temperature corresponding to the thermal voltage generated by the test, indicating that the temperature sensing of the CMTs/KCl/gelatin sensor possessed a high degree of accuracy. This phenomenon was caused by the fact that heat diffusion from human skin raised the temperature of the upper surface of the CMTs/KCl/gelatin sensor. The temperature difference prompted the CMTs/KCl/gelatin sensor to generate a thermal voltage, enabling the sensor to realize non-contact temperature sensing. Thus, the temperature responsiveness of the CMTs/KCl/gelatin sensor provided the potential to detect human body temperature.

Due to its good electrical conductivity and mechanical flexibility, the potential application of CMTs/KCl/gelatin composite in flexible wearable pressure sensor devices was evaluated. Fig. 6(a) shows a diagram of the CMTs/KCl/gelatin pressure sensing test, and its main construction was a sandwich structure of copper foil-CMTs/KCl/gelatin composite-copper foil. The pressure sensing mechanism of the CMTs/KCl/gelatin sensor is shown in Fig. 6(b). As the pressure was increased, the voltage on both sides of the capacitor increased and returned to its original value with the release of pressure. Based on the voltage sensitivity of the CMTs/KCl/gelatin sensor to external forces, different weights were placed on the surface of the CMTs/KCl/gelatin sensor to evaluate its responsiveness and stability to different external forces. As shown in Fig. 6(c), the sensor exhibited a higher voltage response when the load weights were gradually increased from 10 g to 100 g. In addition, the thickness of the CMTs/KCl/gelatin composite had a significant effect

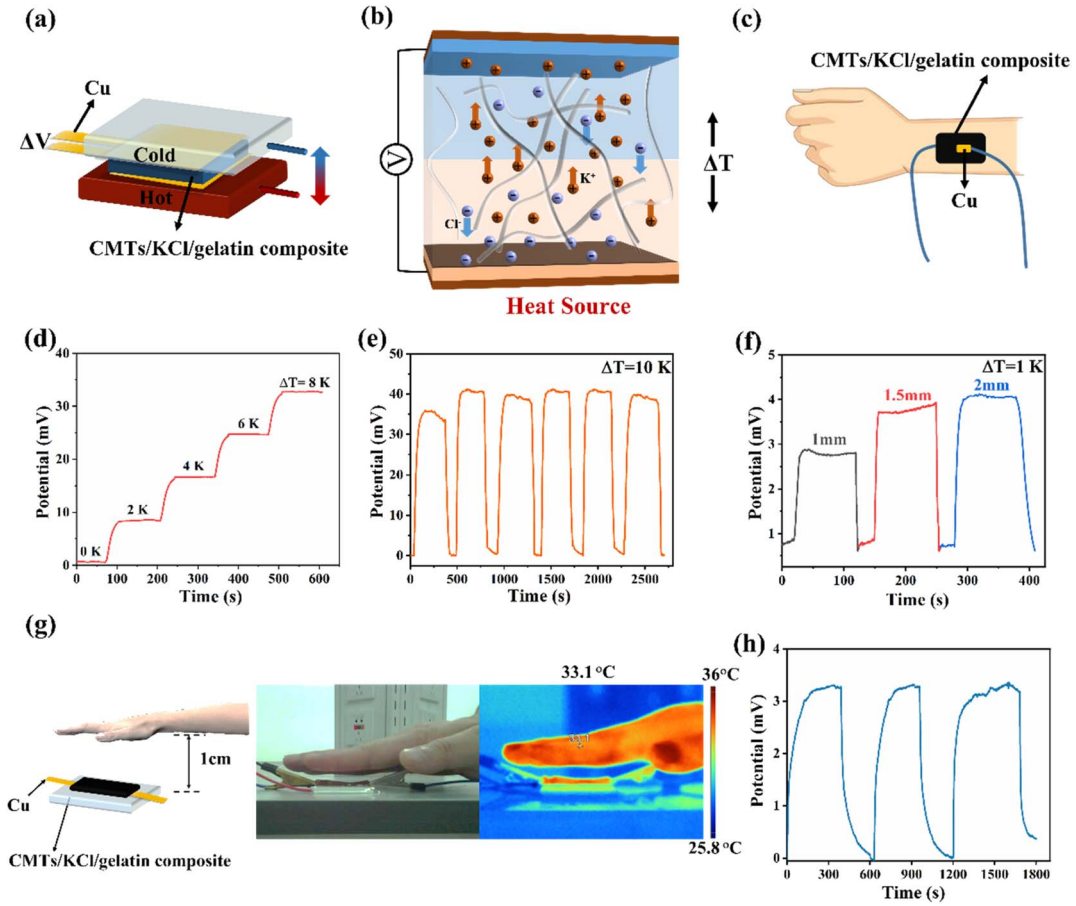

Fig. 5 CMTs/KCl/gelatin sensor temperature sensing test. (a) Schematic diagram of the CMTs/KCl/gelatin temperature sensing test. (b) Diagram of the CMTs/KCl/gelatin temperature sensing mechanism. (c) Schematic diagram of the skin temperature sensing test. (d) Voltage response of the sensor to different temperature differences. (e) Corresponding thermoelectric voltages of the sensor on the skin surface, (f) voltage response of the sensor of different thicknesses to a temperature difference of 1 K. (g) Schematic diagram of the non-contact temperature sensing test and non-contact temperature sensing actual test diagram. (h) Non-contact skin temperature sensing voltage–time curve.

on the sensor performance. The voltage change of the sensor was greater at a load of 100 g for smaller thicknesses in Fig. 6(d). Combining the effects of thickness on temperature sensing and pressure sensing, the 1.5 mm thick CMTs/KCl/gelatin composite was used to assemble with copper foils and adhered to the skin (like fingers and elbows) to examine its ability to monitor human movement in real time.

The CMTs/KCl/gelatin sensor could produce local deformation with the movement of the finger and elbow, leading to the movement of the CMTs in the CMTs/KCl/gelatin composite. The movement of the CMTs changed the internal conductive network of the CMTs/KCl/gelatin composite,[43,44] causing the change in the voltage signals to realize the real-time detection of human body movement. Thus, the voltage signal of the CMTs/KCl/gelatin sensor changes with the movement of the finger and elbow, possessing a good sensitivity in Fig. 6(e) and (f). Moreover, the CMTs/KCl/gelatin sensor displayed regular and effective voltage response signals during repeated bending test of the tester's fingers and elbows. This phenomenon indicated that the CMTs/KCl/gelatin sensor had good pressure sensing capability and possessed a potential in flexible wearable materials.

Furthermore, the responsiveness of the CMTs/KCl/gelatin sensor when used simultaneously as a temperature and pressure sensor was evaluated. As shown in Fig. 6(g), the voltage signal of the sensor displayed a significant change after applying different temperatures on both sides of the sensor and bending the sensor by 90°, indicating that the sensor was capable of responding to both pressure and temperature difference simultaneously in Fig. 6(h). The simultaneous generation of voltage from pressure and temperature difference sensing was greater than the voltage generated by temperature sensing alone in Fig. S5,† indicating that part of the voltage response of the CMTs/KCl/gelatin sensor came from pressure sensing. This phenomenon demonstrated the feasibility of the developed the CMTs/KCl/gelatin sensor for applications in temperature monitoring and pressure sensing. Also, the CMTs/KCl/gelatin sensors were compared with other similar sensors in Table S2.† It could be easily found that the CMTs/KCl/gelatin sensor could simultaneously monitor both temperature and pressure, which was not available in the same type of sensor.

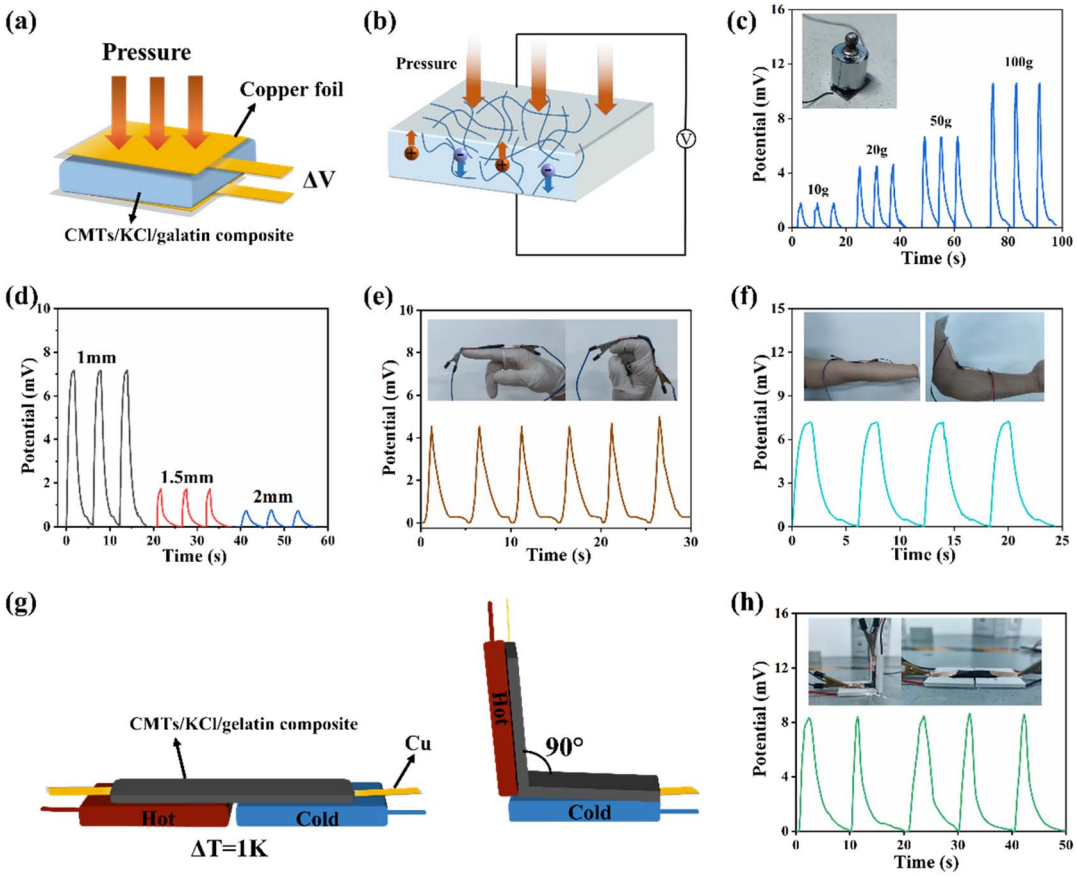

Fig. 6 CMTs/KCl/gelatin sensor pressure sensing test. (a) Schematic diagram of the CMTs/KCl/gelatin pressure sensing test. (b) The pressure sensing mechanism of CMTs/KCl/gelatin sensor. (c) Voltage response of the sensor to different pressures. (d) Voltage response of the sensor with different thicknesses at 100 g weight. (e) Voltage correspondence of the sensor when the finger was bent at 90°. (f) Voltage response of the sensor when the arm was bent. (g) The test schematic of Sensor bending 90°. (h) Voltage response of the sensor when the sensor was bended 90° at a temperature difference of 1 K.

Additionally, all the materials used in the CMTs/KCl/gelatin sensor were cheaper, more readily available, non-toxic to the human body and had a low environmental impact. Overall, such a soft and stretchable CMTs/KCl/gelatin sensor that could monitor both temperature and pressure provided the possibility of broadening flexible wearable sensing devices.

4 Conclusion

In summary, we proposed a flexible stretchable CMTs/KCl/gelatin composite with thermoelectric effect and capability of monitoring temperature and pressure sensing. The as-prepared CMTs/KCl/gelatin composite gave a thermopower of 4 mV K^{-1} and a tensile strength of 1.7 MPa, and it possessed the advantages of flexibility and stretchability, and the responses to both temperature and pressure. In addition, the CMTs/KCl/gelatin sensor can detect temperature differences on the material surface in real-time in both contact and non-contact modes as well as produce a response to a pressure stimulus. When stimulated by both pressure and temperature signals, the CMTs/KCl/gelatin sensor responds to both signals and also detects a voltage significantly higher than that produced by temperature sensing alone. Furthermore, the CMTs/KCl/gelatin sensor can monitor the movement of the human body (fingers, arms) and the temperature difference between the human body and the environment in practical applications. These findings provide a new strategy for the production and utilization of flexible sensors with multi-signal detection.

Conflicts of interest

The authors declare that they have no known competing financial interests or personal relationships that could have appeared to influence the work reported in this paper.

Acknowledgements

The authors are grateful for the support of the Natural Science Foundation of Guangxi (2020GXNSFAA297028), the Project Funded by China Postdoctoral Science Foundation (2017M620361), and the Scientific Research Foundation of Guangxi University (XGZ150513).

References

1 Q. Wang, S. Ling, X. Liang, H. Wang, H. Lu and Y. Zhang, *Adv. Funct. Mater.*, 2019, **29**, 1808695.
2 C.-Y. Tang, X. Zhao, J. Jia, S. Wang, X.-J. Zha, B. Yin, K. Ke, R.-Y. Bao, Z.-Y. Liu, Y. Wang, K. Zhang, M.-B. Yang and W. Yang, *Nano Energy*, 2021, **90**, 106603.
3 W. Lu, P. Yu, M. Jian, H. Wang, H. Wang, X. Liang and Y. Zhang, *ACS Appl. Mater. Interfaces*, 2020, **12**, 11825–11832.
4 L. Gao, Y. Zhang, V. Malyarchuk, L. Jia, K. I. Jang, R. C. Webb, H. Fu, Y. Shi, G. Zhou, L. Shi, D. Shah, X. Huang, B. Xu, C. Yu, Y. Huang and J. A. Rogers, *Nat. Commun.*, 2014, **5**, 4938.
5 Q. Li, L. N. Zhang, X. M. Tao and X. Ding, *Adv. Healthcare Mater.*, 2017, **6**, 1601371.
6 C. Huang, W. Zhang and L. Xue, *Alexandria Eng. J.*, 2022, **61**, 5949–5958.
7 Y. Liu, J. J. S. Norton, R. Qazi, Z. Zou, K. R. Ammann, H. Liu, L. Yan, P. L. Tran, K.-I. Jang, J. W. Lee, D. Zhang, K. A. Kilian, S. H. Jung, T. Bretl, J. Xiao, M. J. Slepian, Y. Huang, J.-W. Jeong and J. A. Rogers, *Sci. Adv.*, 2016, **2**, e1601185.
8 Y. Li, K. Jiang, J. Feng, J. Liu, R. Huang, Z. Chen, J. Yang, Z. Dai, Y. Chen, N. Wang, W. Zhang, W. Zheng, G. Yang and X. Jiang, *Adv. Healthcare Mater.*, 2017, **6**, 1601343.
9 T. Li, F. Liu, X. Yang, S. Hao, Y. Cheng, S. Li, H. Zhu and H. Song, *ACS Appl. Mater. Interfaces*, 2022, **14**, 29261–29272.
10 F. Li, Y. Liu, X. Shi, H. Li, C. Wang, Q. Zhang, R. Ma and J. Liang, *Nano Lett.*, 2020, **20**, 6176–6184.
11 W. D. Li, K. Ke, J. Jia, J. H. Pu, X. Zhao, R. Y. Bao, Z. Y. Liu, L. Bai, K. Zhang, M. B. Yang and W. Yang, *Small*, 2022, **18**, e2103734.
12 H. Zhang, H. Chen, J. H. Lee, E. Kim, K. Y. Chan, H. Venkatesan, M. H. Adegun, O. G. Agbabiaka, X. Shen, Q. Zheng, J. Yang and J. K. Kim, *Adv. Funct. Mater.*, 2022, **32**, 2208362.
13 L. Chen, Y. Xu, Y. Liu, J. Wang, J. Chen, X. Chang and Y. Zhu, *ACS Appl. Mater. Interfaces*, 2023, **15**, 24923–24932.
14 Z. Wu, H. Ding, K. Tao, Y. Wei, X. Gui, W. Shi, X. Xie and J. Wu, *ACS Appl. Mater. Interfaces*, 2021, **13**, 21854–21864.
15 C. Wang, K. Xia, M. Zhang, M. Jian and Y. Zhang, *ACS Appl. Mater. Interfaces*, 2017, **9**, 39484–39492.
16 X. Wu, N. Gao, X. Zheng, X. Tao, Y. He, Z. Liu and Y. Wang, *ACS Appl. Mater. Interfaces*, 2020, **12**, 27691–27699.
17 P. Yang, K. Liu, Q. Chen, X. Mo, Y. Zhou, S. Li, G. Feng and J. Zhou, *Angew Chem. Int. Ed. Engl.*, 2016, **55**, 12050–12053.
18 S. Di Lecce and F. Bresme, *J. Phys. Chem. B*, 2018, **122**, 1662–1668.
19 S. L. Kim, H. T. Lin and C. Yu, *Adv. Energy Mater.*, 2016, **6**, 1600546.
20 B. Kim, J. U. Hwang and E. Kim, *Energy Environ. Sci.*, 2020, **13**, 859–867.
21 H. Wang, D. Zhao, Z. U. Khan, S. Puzinas, M. P. Jonsson, M. Berggren and X. Crispin, *Adv. Electron. Mater.*, 2017, **3**, 1700013.
22 K. M. Liew, Z. X. Lei and L. W. Zhang, *Compos. Struct.*, 2015, **120**, 90–97.
23 D. Mohanta, S. Patnaik, S. Sood and N. Das, *J. Pharm. Anal.*, 2019, **9**, 293–300.
24 N. Behabtu, C. C. Young, D. E. Tsentalovich, O. Kleinerman, X. Wang, A. W. K. Ma, E. A. Bengio, R. F. ter Waarbeek, J. J. de Jong, R. E. Hoogerwerf, S. B. Fairchild, J. B. Ferguson, B. Maruyama, J. Kono, Y. Talmon, Y. Cohen, M. J. Otto and M. Pasquali, *Science*, 2013, **339**, 182–186.
25 X. Li, Y. Tang, J. Song, W. Yang, M. Wang, C. Zhu, W. Zhao, J. Zheng and Y. Lin, *Carbon*, 2018, **129**, 236–244.
26 A. M. Marconnet, M. A. Panzer and K. E. Goodson, *Rev. Mod. Phys.*, 2013, **85**, 1295–1326.
27 W. J. Evans, M. Shen and P. Keblinski, *Appl. Phys. Lett.*, 2012, **100**, 261908.
28 M. Li, Y. H. Sun, B. Dong, H. D. Wu and K. Gao, *Mater. Res. Innovations*, 2015, **19**, 59–63.
29 T. Hayashi and M. Endo, *Composites, Part B*, 2011, **42**, 2151–2157.
30 W. Li, C. Liang, J. Qiu, W. Zhou, H. Han, Z. Wei, G. Sun and Q. Xin, *Carbon*, 2002, **40**, 791–794.
31 S. V. Bulyarskiy, D. A. Bogdanova, G. G. Gusarov, A. V. Lakalin, A. A. Pavlov and R. M. Ryazanov, *Diamond Relat. Mater.*, 2020, **109**, 108042.
32 J. Zhou, Z. Sheng, H. Han, M. Zou and C. Li, *Mater. Lett.*, 2012, **66**, 222–224.
33 H. Haghighi, S. Biard, F. Bigi, R. De Leo, E. Bedin, F. Pfeifer, H. W. Siesler, F. Licciardello and A. Pulvirenti, *Food Hydrocolloids*, 2019, **95**, 33–42.
34 I. Chentir, H. Kchaou, M. Hamdi, M. Jridi, S. Li, A. Doumandji and M. Nasri, *Food Hydrocolloids*, 2019, **89**, 715–725.
35 S. Eigler, C. Dotzer and A. Hirsch, *Carbon*, 2012, **50**, 3666–3673.
36 J. Li, Z. Wang, S. A. Khan, N. Li, Z. Huang and H. Zhang, *Nano Energy*, 2023, **113**, 108612.
37 L. Han, K. Liu, M. Wang, K. Wang, L. Fang, H. Chen, J. Zhou and X. Lu, *Adv. Funct. Mater.*, 2018, **28**, 1704195.
38 D. Aryal and V. Ganesan, *ACS Macro Lett.*, 2018, **7**, 739–744.
39 Y. He, Q. Zhang, H. Cheng, Y. Liu, Y. Shu, Y. Geng, Y. Zheng, B. Qin, Y. Zhou, S. Chen, J. Li, M. Li, G. O. Odunmbaku, C. Li, T. Shumilova, J. Ouyang and K. Sun, *J. Phys. Chem. Lett.*, 2022, **13**, 4621–4627.
40 C.-G. Han, X. Qian, Q. Li, B. Deng, Y. Zhu, Z. Han, W. Zhang, W. Wang, S.-P. Feng, G. Chen and W. Liu, *Science*, 2020, **368**, 1091–1098.
41 T. Li, X. Zhang, S. D. Lacey, R. Mi, X. Zhao, F. Jiang, J. Song, Z. Liu, G. Chen, J. Dai, Y. Yao, S. Das, R. Yang, R. M. Briber and L. Hu, *Nat. Mater.*, 2019, **18**, 608–613.
42 Y. Li, Q. Li, X. Zhang, J. Zhang, S. Wang, L. Lai, K. Zhu and W. Liu, *Energy Environ. Sci.*, 2022, **15**, 5379–5390.
43 M. Amjadi, K.-U. Kyung, I. Park and M. Sitti, *Adv. Funct. Mater.*, 2016, **26**, 1678–1698.
44 Z. Qin, X. Sun, Q. Yu, H. Zhang, X. Wu, M. Yao, W. Liu, F. Yao and J. Li, *ACS Appl. Mater. Interfaces*, 2020, **12**, 4944–4953.